Meccanica (2014) 49:2603–2615
DOI 10.1007/s11012-014-9941-x

Theoretical modeling and analysis of thermal fracture of semi-infinite functionally graded materials with edge cracks

Vera Petrova · Tomasz Sadowski

Received: 13 August 2013 / Accepted: 26 March 2014 / Published online: 10 April 2014

Abstract The present investigation is devoted to a problem of the interaction of two edge cracks inclined arbitrary to the boundary of a non-homogeneous half-plane, which is a functionally graded layer on a homogeneous substrate. The functionally graded properties vary exponentially in thickness direction. One cycle of cooling from sintering temperature is considered. An approach based on integral equations is used and a solution is obtained, then the stress intensity factors are calculated and direction of the initial crack propagation is evaluated by using the maximum circumferential stress criterion. Influence of geometrical and material (inhomogeneity) parameters on the fracture characteristics is investigated. This study can serve as a part of the modeling of the fracture process in FGM coatings under cyclic heating–cooling thermal loading.

Keywords Edge cracks · Singular integral equations · Stress intensity factors · Thermal fracture

V. Petrova
Voronezh State University, University Sq. 1,
Voronezh 394006, Russia
e-mail: veraep@gmail.com

T. Sadowski (✉)
Lublin University of Technology, Nadbystrzycka 40,
20-618 Lublin, Poland
e-mail: t.sadowski@pollub.pl

1 Introduction

In different engineering applications, e.g., nuclear energy, aerospace, energy conversions, thermal barrier coating are used to protect metallic or composite components from extremely high temperatures [1–3]. Last years for these purposes the so-called functionally graded materials (FGMs) are used. FGMs are composite materials with continuously varying properties in one direction. The application of FGM coatings can reduce bimaterial mismatch at interfaces between the coating and the substrate and prevent delamination and debonding along interfaces. However, cracks can initiate from initial defects or microcracks appear during manufacturing or service. Experimental results [4] showed that when functionally graded plates are subjected to thermal shock, multiple cracks often occur on the ceramic surface during cooling-heating cycles. This fracture process begins from formation of a single crack from initial defects and then a system of edge cracks is formed. Therefore, the study of fracture of FGM coatings is important for a better understanding of the fracture processes in FGM structures and to improve their fracture resistance.

Numerous papers are devoted to different problems of modelling and analysis of fracture processes in FGMs, references can be found in the review papers [2, 5]. Different methods are widely used for modeling of FGMs and structures under thermal and mechanical loadings, among them FE methods [6–8], the

boundary integral methods [9–14] and their modifications [15, 16]. In spite of many available solutions the problems of interaction of arbitrary located cracks in FGMs are still important.

An approximation method for determining stress intensity factors for a periodic system of edge cracks in an FGM coating in a semi-infinite medium was introduced in [9]. The method is based on singular integral equations. The validity of this approach is discussed in [17] and good accuracy is demonstrated for some gradient (inhomogeneity) parameters of FGMs and crack lengths.

The present work is devoted to the theoretical modeling of fracture of a FGM coating on a semi-infinite homogeneous substrate under thermal and mechanical loading. One cycle of cooling from sintering temperature is considered. It is supposed that two edge cracks arbitrary inclined to the boundary are located in the FGM. The FGM properties are presented by exponential functions. The method of singular integral equations is used and approach similar to the presented in [9] is applied. It is supposed that the inhomogeneity of material is revealed in non-homogeneous residual stresses on crack surfaces. An example of accounting such residual forces can be found in [9] where a semi-infinite functionally graded material (FGM) with edge cracks is considered. In [18] the influence of an additional loading, which varies with a coordinate along the crack line (and can be considered as a residual stress), on both stress intensity factors Mode I and Mode II was considered in the problem for two parallel cracks under shear loading (pure Mode II) corresponding to the loading in a Compact Shear specimen. In the present investigation the interaction of two edge cracks is considered and this study can serve as a part of the modeling of the fracture process in FGM coatings and further formation of a system of cracks under cyclic thermal loading.

2 Formulation of the problem

The present investigation is devoted to a problem of the interaction of two edge cracks (with length $2a_n$, $n = 1, 2$) inclined arbitrary to the boundary of a non-homogeneous half-plane (Fig. 1). Cartesian coordinates (x,y) have x-axis along the boundary of the half-plane, local coordinate systems (x_n, y_n) are attached to each crack. The crack position is determined by the crack midpoint coordinate $z_n^0 = x_n^0 + iy_n^0$ ($i = \sqrt{-1}$ is the imaginary unity) and an inclination angle β_n to the boundary, i.e. to the x-axis (Fig. 1).

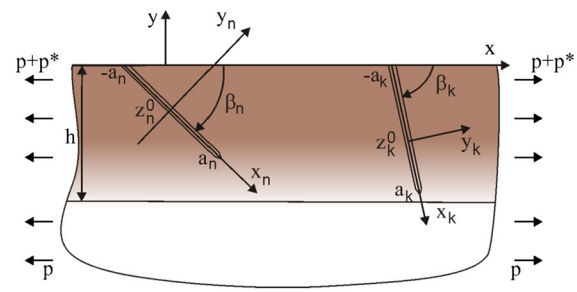

Fig. 1 Two edge cracks in a non-homogeneous half-plane

A functionally graded material (FGM) is located in the region $0 \le y \le -h$ with width h. The Poisson's ratio v is assumed to be a constant because the effect of its variation on the crack-tip stress intensity factors is negligible [19, 20]. The remaining thermo-mechanical properties, i.e. the Young's modulus $E(y)$ and the coefficient of thermal expansion $\alpha_t(y)$, depend on the y-coordinate only and are modeled by the exponential function [12–14, 19, 20].

For arbitrary located cracks in a half-plane the system of singular integral equations is written as [21, 22].

$$\int_{-a_n}^{a_n} \frac{g_n'(t)dt}{t-x} + \sum_{\substack{k=1 \\ k\neq n}}^{N} \int_{-a_k}^{a_k} [g_k'(t)R_{nk}(t,x) + \overline{g_k'(t)}S_{nk}(t,x)]\,dt = \pi p_n(x), \quad |x| < a_n,\ n = 1,2 \tag{1}$$

and for two cracks we have two equations. N is the number of cracks, i.e. $N = 2$ is in our case. The unknown functions

$$g_n'(x) = \frac{2\mu}{i(\kappa+1)} \frac{\partial}{\partial x}([u_n] + i[v_n]) \tag{2}$$

are the derivative of displacement jumps on the crack faces; $[u_n]$ and $[v_n]$ are shear and vertical displacement jumps, respectively, on the n-th crack line, $\mu = E/2(1+v)$is the shear modulus, E—the Young's modulus, v—the Poisson's ratio, $\kappa = 3 - 4v$—for the plane strain state and $\kappa = (3-v)/(1+v)$—for the plane stress state.

The functions p_n are determined by the applied load. The regular kernels R_{nk}(t,x) and $S_{nk}(t,x)$ contain geometry of the problem and are cited in the "Appendix" in Eqs. (22)–(26).

Equations (1) and (2) are for common case of two arbitrary cracks in a half plane. For edge cracks we should put $z_n^0 = x_n^0 - ia_n \sin\beta_n$.

The FGM is cooled from sintering temperature. The FGMs inhomogeneity is accounted via continuously varying residual stresses arising due to mismatch in the coefficients of thermal expansion. The additional stresses p^* are the following [9]:

$$p^*: \quad \sigma_{xx}^T(y) = [\alpha_t(y) - \alpha_{t0}]\Delta TE(y), \quad \sigma_{xx}^e(y) = [E(y)/E_0 - 1]\sigma_{xx}^0. \tag{3}$$

These functions will be added to the right side of Eq. (1). α_{t0} is the thermal expansion coefficient of a homogeneous material (in the region $y < -h$) and E_0 is the Young's modulus of this material.

The thermal expansion coefficient of the FGM layer is presented in the exponential form

$$\alpha_{t1} = \alpha_{t0}\exp(\varepsilon(y+h)), \quad -h \le y \le 0, \tag{4}$$

where ε is the inhomogeneity parameter of this coefficient. The Young's modulus is

$$E = E_0\exp(\delta(y+h)), \quad -h \le y \le 0 \tag{5}$$

with the inhomogeneity parameter δ. This exponential model describes the smooth variation of material properties of the FGM in the y-axis direction. For example, if α_{t1} is decreased with increasing y-coordinate (from $y = -h$ to $y = 0$), then the inhomogeneity parameter ε is negative, and this case can correspond to a ceramic/metal FGM layer on a metal substrate with gradual transition from a metal at $y = -h$ to a ceramic at the upper part of the FGM layer ($\alpha_{t1}^{ceramic} < \alpha_{t1}^{metal}$).

The relation between the global coordinates (x,y) and the local coordinate systems (x_k,y_k) can be written in the complex form as follows $z = z_k^0 + z_k e^{-i\beta_k}$, where $z_k = x_k + iy_k$ and $i = \sqrt{-1}$. $z_k^0 = x_k^0 + iy_k^0$ is the origin coordinate of the system (x_k,y_k) in the global system. In the local coordinate system (x_k,y_k) connected with each crack the coefficient α_{t1} Eq. (4) possesses the form

$$\alpha_{t1}(x_k,y_k) = \alpha_{t0}e^{\varepsilon(h+y_k^0)}e^{\varepsilon_1 x_k + \varepsilon_2 y_k}, \ \varepsilon_1 = \varepsilon\ \sin(-\beta_k),\ \varepsilon_2 = \varepsilon\ \cos\beta_k$$

and on the crack lines, where $y_k = 0$, we will have

$$\alpha_t = \alpha_{t0}\exp(\varepsilon(h + y_k^0))\exp(-\varepsilon x_k \sin\beta_k) \tag{6}$$

Similar expressions can be written for the Young's modulus.

If we suppose that the Young's moduli of materials in the FGM have approximately same values, then in this case—$\sigma_{xx}^e(y) = 0$ in Eq. (3). It means that the material is elastically homogeneous. Examples of such materials are the following: ceramic/ceramic TiC/SiC, $MoSi_2/Al_2O_3$ and $MoSi_2$/SiC, and also ceramic/metal FGMs, e.g., zirconia/nickel and zirconia/steel. For this special case we will investigate the influence of the inhomogeneity parameter ε on the fracture characteristics of the materials. For a fully non-homogeneous material we will have two inhomogeneity parameters ε and δ.

Equations (1) and (2) are rewritten in dimensionless form with the non-dimension coordinates $\xi = t/a$ and $\eta = x/a$, where $2a$ is a length of the crack (here we suppose that $a_1 = a_2 = a$). In the considered case of the edge cracks functions $g_n'(\eta)$ are bounded in the edge point, i.e. at the point $\eta = -1$. At the other tip of the crack, for $\eta = 1$, the functions $g_n'(\eta)$ as well as the stresses have the square root singularity. The stress intensity factors (SIFs) at the internal tips of the edge cracks are obtained as

$$K_{nI} - iK_{nII} = -\lim_{\eta\to+1}\sqrt{a}\sqrt{1-\eta^2}\,g_n'(\eta)\ (n = 1,2). \tag{7}$$

3 Solution

3.1 Numerical solution

The system of Eq. (1) is solved by the method of mechanical quadrature [21–23] which is based on the Chebyshev polynomials. The solution for edge cracks is presented in the following form

$$g_n'(\eta) = u_n(\eta)/\sqrt{1-\eta^2} \tag{8}$$

Here $u_n(\eta)$ are regular functions on the segment [−1,1] and $1/\sqrt{1-\eta^2}$ is the weight function. Condition that the functions $g_n'(\eta)$ are bounded at the edge point $\eta = -1$ (or have a singularity less than $1/\sqrt{1+\eta}$) is the following [22]

$$u_n(-1) = 0. \tag{9}$$

That is the exact singularity at the edge points is not taking into account, but the result obtained with this assumption has shown good accuracy [22].

Using Gauss's quadrature formulae for the regular and the singular integrals the integral equations are reduced to the system of $N \times M$ ($N = 2$—number of cracks, M—number of nodes) algebraic equations

$$\frac{1}{M}\sum_{m=1}^{M}\sum_{k=1}^{N}\left[u_k(\xi_m)R_{nk}(\xi_m,\eta_r)+\overline{u_k(\xi_m)}S_{nk}(\xi_m,\eta_r)\right] = \pi p_n(\eta_r), \tag{10}$$

$$\sum_{m=1}^{M}(-1)^m u_n(\xi_m)\tan\frac{2m-1}{4M}\pi = 0 \ (n=1,2; r=1,2,\ldots,M-1) \tag{11}$$

where

$$\xi_m = \cos\frac{2m-1}{2M}\pi \ (\mathrm{m}=1,2,\ldots,\mathrm{M}); \quad \eta_r = \cos\frac{\pi r}{M} \ (r=1,2,\ldots,\mathrm{M}-1) \tag{12}$$

M is the total number of the discrete points of the unknown functions $u_n(\eta)$ on the interval (−1,1). After solution of the algebraic system (10) and (11) the functions $u_n(\eta)$ are calculated by the interpolation formula:

$$u_n(\eta) = \frac{2}{M}\sum_{m=1}^{M}u_n(\xi_m)\sum_{r=0}^{M-1}T_r(\xi_m)T_r(\eta) - \frac{1}{M}\sum_{m=0}^{M}u_n(\xi_m). \tag{13}$$

Here T_r are the Chebyshev polynomials of the first kind. Setting $\eta = 1$ in Eq. (13), it is obtained

$$u_n(+1) = \frac{1}{M}\sum_{m=1}^{M}(-1)^{m+1}u_n(\xi_m)\cot\frac{2m-1}{4M}\pi \tag{14}$$

and for $\eta = -1$ we have

$$u_n(-1) = \frac{1}{M}\sum_{m=1}^{M}(-1)^{M+m}u_n(\xi_m)\tan\frac{2m-1}{4M}\pi$$

This equation and the condition (9) yield Eq. (11).

Applying the conjugate operation to the system (9) additional $N \times M$ equations are obtained, i.e. $2N \times M$ equations should be solved, for two cracks we have $4 \times M$ equations.

Inserting Eq. (14) into the formula (8) and then into Eq. (7) the SIFs are obtained

$$K_{In} - iK_{IIn} = -\sqrt{a_n}u_n(+1) \ (n=1,2). \tag{15}$$

3.2 Validation

To validate this model and verify computational results, we consider some numerical examples and compare our results for SIFs with other available in the literature. The validation of the approximation method similar to the present method with respect to stress intensity factors was discussed in [17]. It was shown that the error depends on the gradient of the profile of Young's modulus of FGMs and crack lengths. For a small crack length the error remains within acceptable limits even for a large gradient (a large inhomogeneity parameter) at the crack tip. However, for a large crack length the gradient (inhomogeneity parameter) should be small at the crack tip for the error to be small. In our modeling the inhomogeneity parameters are used in the range from −1 to 1.

For verification of the numerical results and validation of the computer program a particular case of two inclined edge cracks in a homogeneous half-plane under uniform tension p (Fig. 1, $p^* = 0$) is considered. The cracks are assumed to have same length $2a_i = 2a$ and same slope angle β. Distance between the cracks we denote by $\hat{d}$ and the non-dimensional distance by $d = \hat{d}/a$. The numerical results with respect to the stress intensity factors are obtained for different angles β in the range of 15° to 90° and for different non-dimensional distances d between the cracks. The SIFs Mode I (K_I) and Mode II (K_{II}) are presented in the non-dimensional form $k_{I,II} = K_{I,II}/K^0$, they are normalized by $K^0 = p\sqrt{2a}$.

The convergence of the numerical results is checked by comparing the values for SIFs for different number of collocation points M. In the case of the angle β = 90° M = 40 is enough for good accuracy, the results obtained for M = 40 and M = 80 are very close, they differ only in forth sign in the decimal digit, the relative error is about 10^{-2}. At the same time for 15° similar good accuracy can be achieved for M = 80. For the problem of a single oblique edge crack under constant normal tractions applied to the crack surfaces the results showed good accuracy for M = 30 and good agreement with the results cited in [21, 22] is demonstrated.

Table 1 Non-dimensional SIFs (k_I, k_{II}) of the edge cracks in a semi-infinite homogeneous plane

d	β					
	15°	30°	45°	60°	75°	90°
1 [25]	0.134; 0.157	0.263; 0.258	0.418; 0.323 0.28; 0.18	0.582; 0.332	0.725; 0.275	0.817; 0.159
10 [25]	0.229; 0.224	0.448; 0.328	0.667; 0.352 0.67; 0.35	0.855; 0.298	0.986; 0.179	1.037; 0.019
60	0.232; 0.227	0.462; 0.336	0.704; 0.364	0.918; 0.305	1.066; 0.173	1.118; 0.000
100						1.121; 0.000
[10]	0.232; 0.226	0.462; 0.336	0.705; 0.365	0.920; 0.306	1.069; 0.174	1.121; 0.000

Table 2 Thermal properties of some FGMs and the inhomogeneity coefficient ε

Thermal expansion coeff. ($*10^{-6}$ K^{-1})				Thermal conductivity ($Wm^{-1}K^{-1}$)	
FGM/H (Al_2O_3/$MoSi_2$)/$MoSi_2$ (Ceramic/Ceramic)					
Al_2O_3	α_{t1}	5	$\alpha_{t1}/\alpha_{t2} = 1$	k_1	25
$MoSi_2$	α_{t2}	5	$\varepsilon = 0$	k_2	52
FGM/H ($MoSi_2$/Al_2O_3)/Al_2O_3	$\varepsilon = 0$				
FGM/H ($MoSi_2$/SiC)/SiC (Ceramic/Ceramic)					
$MoSi_2$	α_{t1}	5	$\alpha_{t1}/\alpha_{t2} > 1$	k_1	52
SiC	α_{t2}	4	$\varepsilon > 0$	k_2	60
FGM/H (SiC/$MoSi_2$)/$MoSi_2$	$\varepsilon < 0$				
FGM/H (TiC/SiC)/SiC (Ceramic/Ceramic)					
TiC	α_{t1}	7	$\alpha_{t1}/\alpha_{t2} > 1$	k_1	20
SiC	α_{t2}	4	$\varepsilon > 0$	k_2	60
FGM/H (SiC/TiC)/TiC	$\varepsilon < 0$				
FGM/H (ZrO_2/Ni)/Ni (Ceramic/Metal)					
ZrO_2	α_{t1}	10	$\alpha_{t1}/\alpha_{t2} < 1$	k_1	2
Ni	α_{t2}	18	$\varepsilon < 0$	k_2	90
FGM/H (Ni/ZrO_2)/ZrO_2	$\varepsilon > 0$				
FGM/H (ZrO_2/Steel)/Steel (Ceramic/Metal)					
ZrO_2	α_{t1}	10	$\alpha_{t1}/\alpha_{t2} < 1$	k_1	2
Steel	α_{t2}	12	$\varepsilon < 0$	k_2	20
FGM/H (Steel/ZrO_2)/ZrO_2	$\varepsilon > 0$				

Comparison with published in the literature solutions for SIFs can be done for the homogeneous half-plane. The values for SIF for oblique edge cracks can be found in [10, 21–25]. Detailed analysis of these problems was done for one crack in [10] and for periodic edge cracks of unequal cracks in a semi-infinite tensile sheet in [25] for $\beta = 45°$. Unfortunately, the results for SIFs for two oblique edge cracks by Nisitani 1977 cited in the handbook of Murakami [24] are not clear for comparison with our results (besides, the original paper by Nisitani 1977 is not available). The comparison have been done with results for SIFs for a single inclined edge crack cited in [10] and with SIFs for periodic edge cracks cited in [25]. Table 1 shows that with increasing the distance d between the cracks the SIF tends to the value for a single edge crack cited in [10]. It should be noted that for the small slope angles $\beta = 15°$ and 30° and for the distance for $d = 10$ the values of SIFs are close to the values of SIFs for a single edge crack [10]. With increasing the angle β larger distances d should be taken to achieve the same

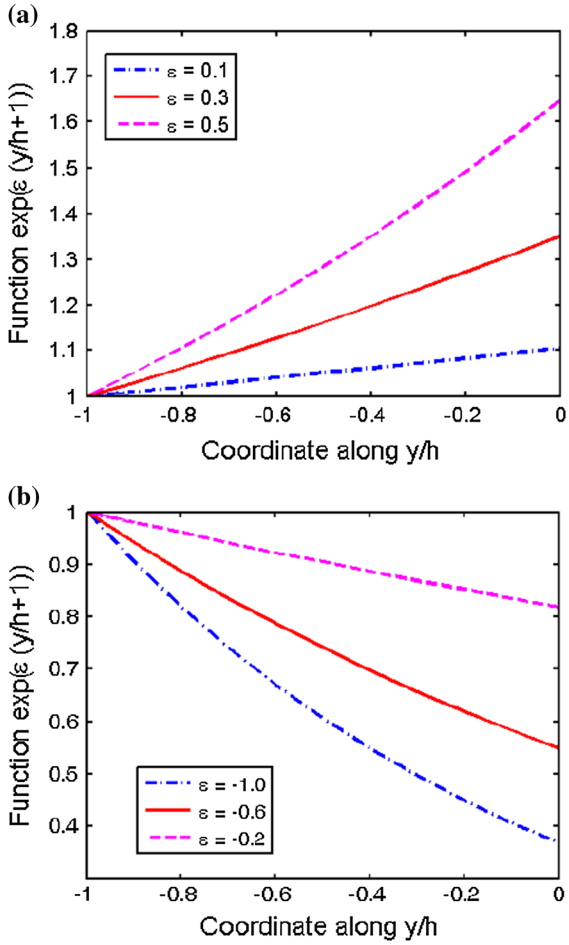

Fig. 2 Variation of the exponential function in Eq. (1) with non-dimensional coordinate y/h: **a** for positive ε, **b** for negative ε

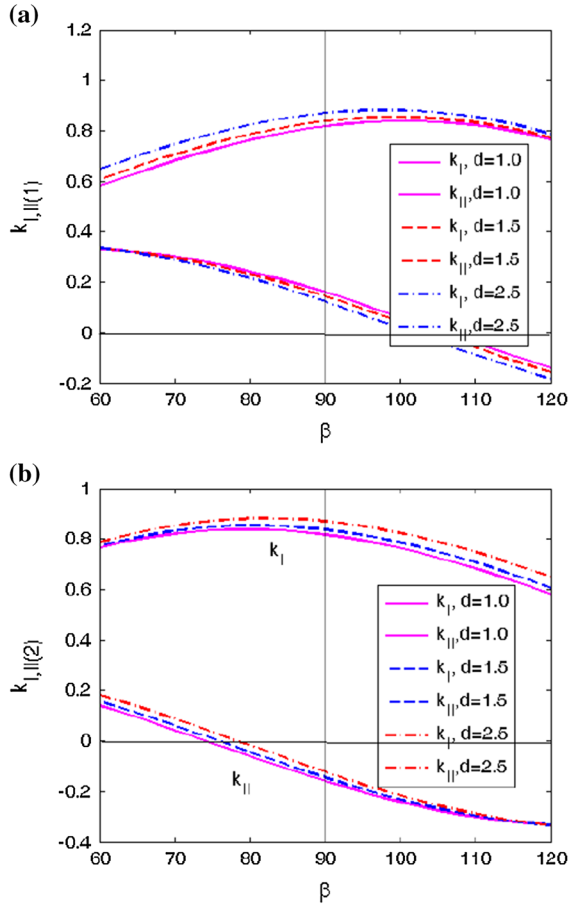

Fig. 3 SIFs k_I and k_{II} as function of the angle β ($\beta_n = \beta$, n = 1, 2) for two edge cracks: **a** for crack 1, **b** for crack 2. Homogeneous material

result, e.g., for $\beta = 90°$ good result is for the distance $d = 100$. It means that for small inclination angles ($\beta = 15°$ and 30°) the interaction between a half-plane boundary and cracks is stronger than the interaction between the cracks.

Comparison of the values for SIFs for two interacting edge cracks with the SIFs [25] for a crack in a periodic system of edge cracks inclined on the angle $\beta = 45°$ shows that the values of SIFs are similar for $d = 10$ and differ considerably for close located cracks with $d = 1$, see Table 1.

For all angles β the SIF k_I increases with increasing the distance d between the cracks and tends to the value for a single crack, while with decreasing d the SIF k_I decreases, i.e. the so-called shielding effect is observed which is known for the parallel cracks under tension normal to the crack lines. Behavior of k_{II} is more complicated than k_I. For the angles $\beta = 15°, 30°$, 45° and 60° k_{II} increases with increasing the distance between the cracks, and for $\beta = 75°$ and 90° k_{II} decreases.

4 Results

4.1 Material parameters

For analysis of the fracture development in an FGM/homogeneous half plane with pre-existing two edge cracks the parameters of the materials should be chosen. Besides, a model for the functional gradation has to be selected. In this study the exponential form for FGMs is used, Eqs. (4)–(6). Then, on the basis of this model and real material combinations of the

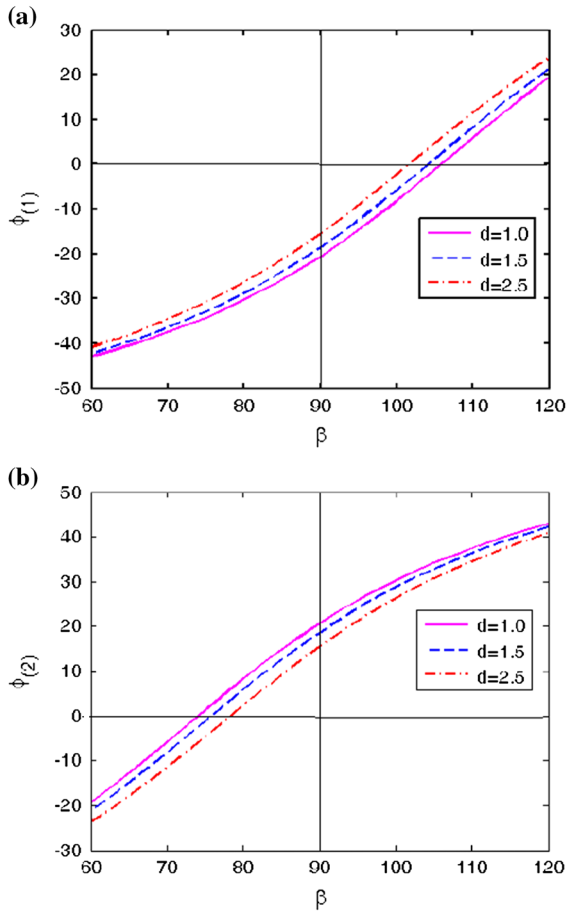

Fig. 4 Fracture angles as function of the angle β ($\beta_n = \beta$, n = 1, 2) for two edge cracks: **a** for crack 1, **b** for crack 2. Homogeneous material

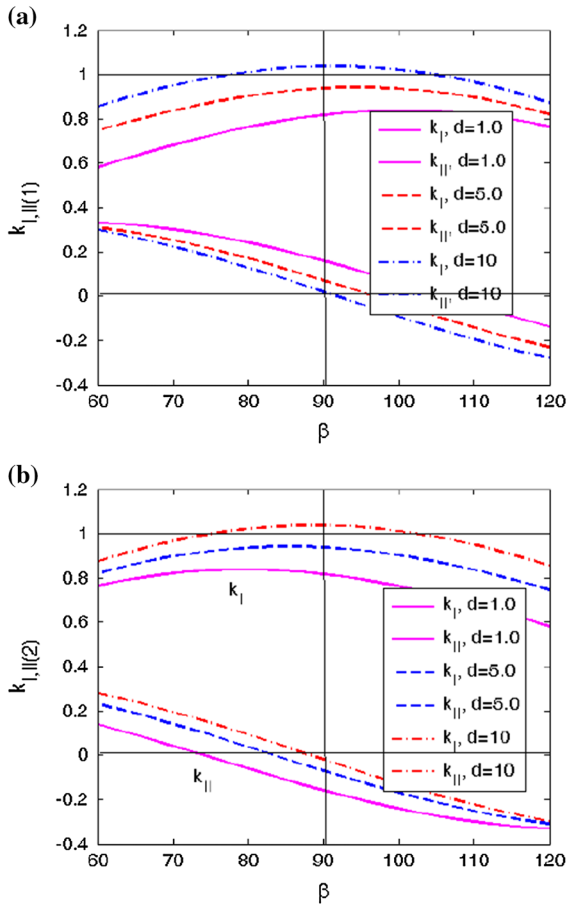

Fig. 5 SIFs k_I and k_{II} as function of the angle β ($\beta_n = \beta$, n = 1, 2) for two edge cracks: **a** for crack 1, **b** for crack 2. Homogeneous material

structure the special inhomogeneity parameters should be estimated.

Functionally graded materials are used in thermal barrier coating to protect details from high temperatures as well as from wear and corrosion. The materials for protecting from high temperatures should have a low thermal conductivity and at the same time they are desired to have a thermal expansion coefficient close to that of the material for the protected substrate. Consider some actual material combinations ceramic/ceramic and ceramic/metal which can be used in the model. The parameters of these materials, which are available in the literature, are presented in the Table 2 [26]. The Young's modules of these materials are similar; it means that these FGMs are elastically homogeneous, in this case—$\sigma^e_{xx}(y) = 0$ in Eq. (3). For this special case we can investigate the influence of the inhomogeneity parameter ε on the fracture characteristics of the material, such as the stress intensity factors at crack tips and the fracture angles which determine the direction of further propagation of cracks.

From Eq. (4) $\alpha_{t1}/\alpha_{t0} = \exp(\varepsilon(y + h))$ and the inhomogeneity parameter ε is written as

$$\varepsilon = \ln(\alpha_{t1}/\alpha_{t0})/(y + h). \tag{16}$$

Equation (16) in combination with data in Table 2 shows that the values of ε for a thick FGM layer are not large and, accordingly, the actual variation of the residual stresses with coordinate y is not very strong. Figure 2 illustrates the variations of exponential functions $\exp(\varepsilon(y/h + 1))$ with the non-dimensional

coordinate y/h for different parameters ε, positive at Fig. 2a and negative at Fig. 2b. Here ε denotes the non-dimensional εh. The value of the exponential function (and, hence, the other values, containing this function, e.g., the thermal expansion coefficient and residual stresses) increases by 35 % for $\varepsilon = 0.3$ and decreases by the same value for the negative ε equals to $\varepsilon = -1$.

4.2 Stress intensity factors and fracture angles

To study the effects of inhomogeneity parameters of FGMs on the SIFs at the tips of the edge cracks, as well as on the other fracture characteristic, such as fracture angles, some examples for the problem with respect to loading, material parameters and geometry are considered.

The direction of the initial crack propagation (fracture angle) is evaluated by using the maximum circumferential stress criterion (Cherepanov 1963; Erdogan and Sih 1963; Panasyuk and Berezhnitskij 1964, see for the references [27]) and is written as

$$\phi_0 = 2\,\mathrm{arctg}\left[\left(K_I - \sqrt{K_I^2 + 8K_{II}^2}\right)/4K_{II}\right] \qquad (17)$$

For cracks in pure Mode II loading ($K_I = 0$) the fracture angle is calculated as $|\phi_0| \approx 70.5^{\circ}$. For elastically homogeneous materials we can use this criterion without any assumptions. In the case of an elastically non-homogeneous material it is supposed that the material is elastically homogeneous in a vicinity of the crack tips.

We will suppose that the cracks have equal lengths $a_1 = a_2 = a$ and the same inclination angles $\beta_1 = \beta_2 = \beta$ to the boundary. These assumptions are made for simplicity of the parametric analysis. Other crack geometries will be studied in other future works.

4.2.1 Two edge cracks in a homogeneous half-plane

For this case we have only tensile loading p parallel to the boundary of the half-plane, which corresponds to the function

$$p_n = \sigma_n - i\tau_n = p(1 - \exp(-2i\alpha_n))/2 \ (n = 1, 2) \qquad (18)$$

in the integral Eqs. (1) and (9), here $\alpha_n = -\beta_n$. The non-dimensional SIFs ($k_{I,II} = K_{I,II}/\sigma\sqrt{2a}$) Mode I and Mode II and the fracture angles Eq. (18) are presented in Figs. 3, 4, 5, 6. Variation of these values with the inclination angle $60^{\circ} \le \beta \le 120^{\circ}$ of the cracks to the half-plane boundary is shown for different distances between the cracks: Figs. 3 and 4 for $d = 1, 1.5, 2.5$, and Figs. 5 and 6 for $d = 1, 5, 10$.

Small variation of the magnitude of k_I with changing β is observed in Fig. 3 and $k_I < 1$ for all β and d, hence k_I is smaller than k_I for a solitary crack and the shielding effect is observed. The SIF k_{II} decreases with increasing β from 60° to 120° and changes the sign at $\beta \approx 105^{\circ}$ for the crack 1 and at $\beta \approx 75^{\circ}$ for the crack 2. It means also that at these angles we have pure mode conditions. Figure 4 shows that the fracture angles increases with increasing β and change orientation (sign) at $\beta \approx 105^{\circ}$ for the crack 1

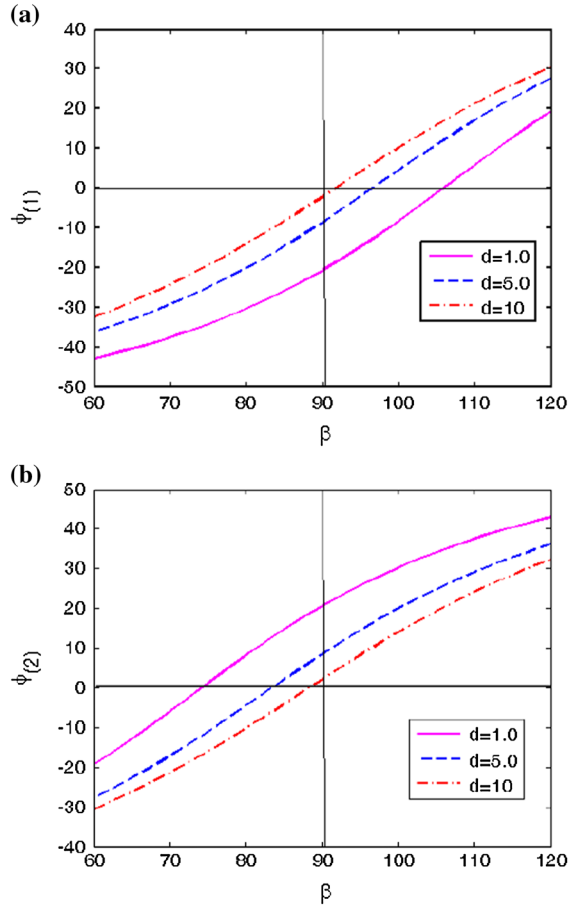

Fig. 6 Fracture angles as function of the angle β ($\beta_n = \beta$, n = 1, 2) for two edge cracks: **a** for crack 1, **b** for crack 2. Homogeneous material

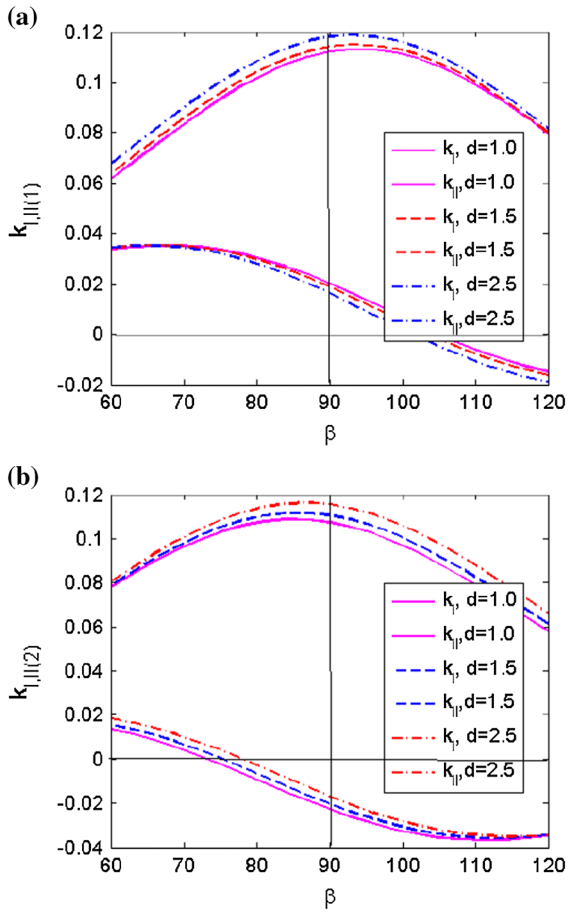

Fig. 7 SIFs k_I and k_{II} as function of the angle β ($\beta_n = \beta$, n = 1, 2) for two edge cracks: **a** for crack 1, **b** for crack 2; for $\varepsilon a = -1$. Thermo-mechanical loading, $E = E_0$

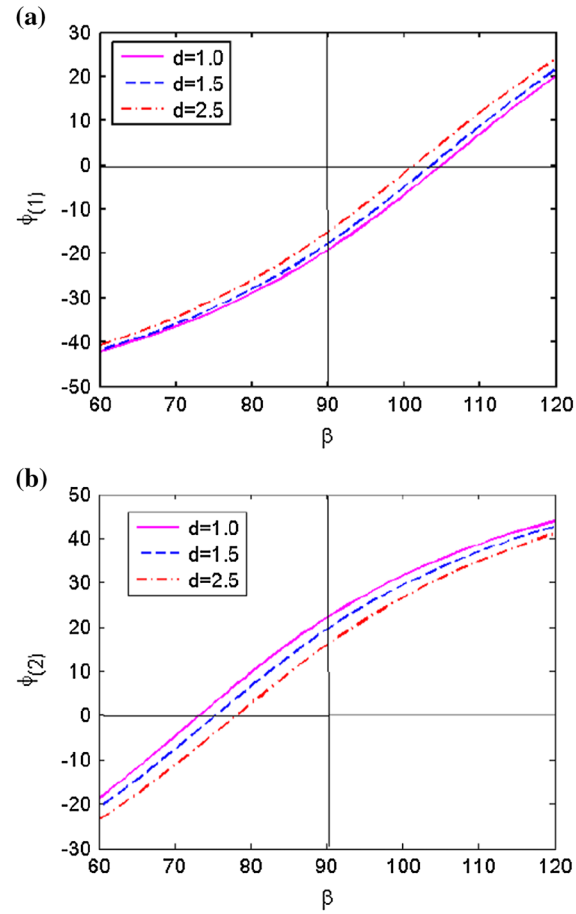

Fig. 8 Fracture angles as function of the angle β ($\beta_n = \beta$, n = 1, 2) for two edge cracks: **a** for crack 1, **b** for crack 2; for $\varepsilon a = -1$. Thermo-mechanical loading, $E = E_0$

(Fig. 4a) and at $\beta \approx 75°$ for the crack 2 (Fig. 4b) and it corresponds to the change of the sign of k_{II}, which characterizes the fracture angles in mixed-mode conditions.

For close located cracks ($d = 1,\ 1.5,\ 2$) the influence of d on k_I and k_{II} is small (Fig. 3) but for $d = 1,\ 5,\ 10$ this influence is stronger (Fig. 5). For $d = 10$ and $\beta \approx 90°$ $k_I > 1$, i.e. greater than k_I for a single crack in an infinite plane and close to the value k_I for a single edge crack.

4.2.2 *Elastically homogeneous material*

It was mentioned above that $E = E_0$ and $\sigma^e_{xx}(y) = 0$ for this case and, hence, Eq. (3) is written as

$$p^* = \sigma^T_{xx}(y) = [\alpha_t(y) - \alpha_{t0}]\Delta T E(y)$$
$$p + p^* = Q[p/Q + [\exp(\varepsilon(h + y^0_k))\exp(-\varepsilon x_k \sin\beta_k) - 1]]$$
$$Q = \alpha_{t0}\Delta T E_0 \qquad (19)$$

If we suppose that $p = Q$, i.e. mechanical and thermal loadings are equal, then

$$p + p^* = Q\ \exp(\varepsilon(h + y^0_k))\exp(-\varepsilon x_k \sin\beta_k) \qquad (20)$$

Otherwise the new parameter p/Q should be considered. In the right side of Eqs. (1) and (10) the function (18) with p determined by (20) should be used.

For elastically inhomogeneous materials under tension (without thermal loading, i.e. for $\sigma^T_{xx}(y) = 0$) the load (3) will be determined by the same expressions (19) and (20), where instead of the thermal load Q will be the mechanical load p.

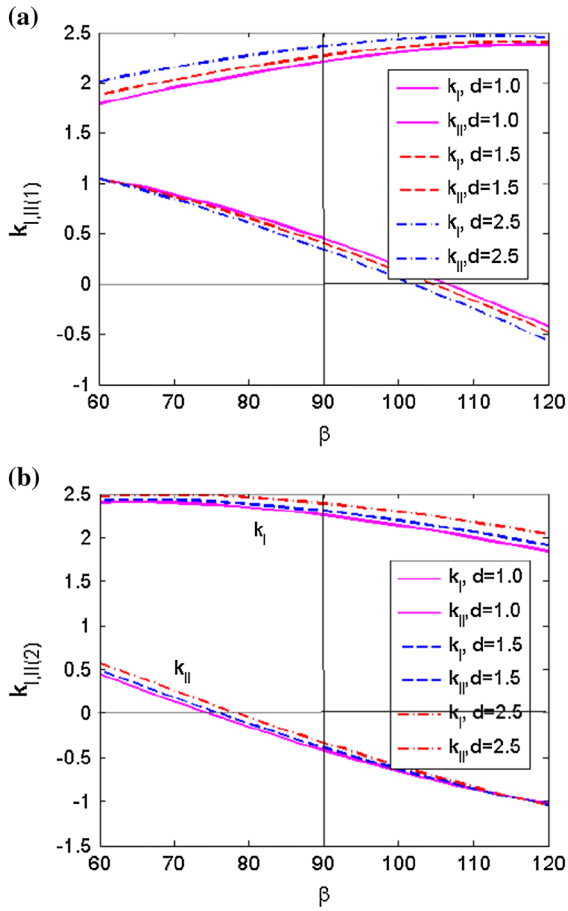

Fig. 9 SIFs k_I and k_{II} as function of the angle β ($\beta_n = \beta$, n = 1, 2) for two edge cracks: **a** for crack 1, **b** for crack 2; for $\varepsilon a = 0.5$. Thermo-mechanical loading, $E = E_0$

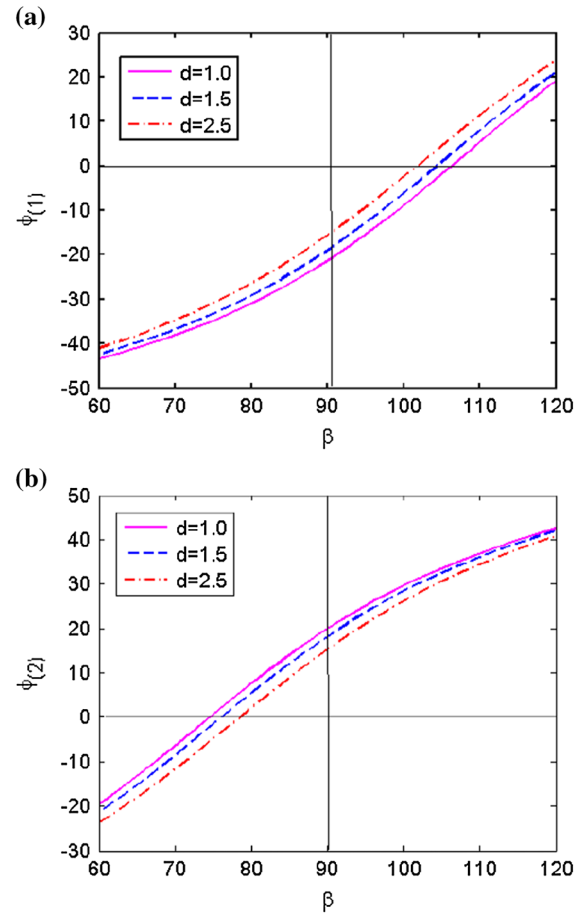

Fig. 10 Fracture angles as function of the angle β ($\beta_n = \beta$, n = 1, 2) for two edge cracks: **a** for crack 1, **b** for crack 2; for $\varepsilon a = 0.5$. Thermo-mechanical loading, $E = E_0$

In the numerical results the inhomogeneity parameter ε is used in the non-dimensional form εa (here a is half size of a crack).

Figures 7, 8, 9, 10 show the results of calculation of SIFs and the fracture angles (the maximum circumferential stress criterion was used) for two edge cracks. For this case of thermally non-homogeneous materials we have only one inhomogeneity parameter εa of the thermal expansion coefficient. The SIFs are presented in the non-dimensional form $k_{I,II} = K_{I,II}/Q\sqrt{2a}$. The calculation were performed for the non-dimensional distances $d = 1$, 1.5, 2.5 and the non-dimensional $h/a = 4$. Two values of the inhomogeneity parameter are used $\varepsilon a = -1$ and 0.5. The result is obtained on the basis of the solution of the system (10)–(11) for a special case where at the right side of Eq. (1) and accordingly in Eq. (9) is the function (18) with (20).

Figures 7 and 8 show k_I, k_{II} and the fracture angles ϕ as functions of β for $\varepsilon a = -1$, which corresponds to smaller value of the thermal expansion coefficient in the upper part of the FGM layer. Comparing this case and the previous homogeneous case we see similar trends in the results, but with some non-linearity and with different magnitudes. The values of k_I, k_{II} and ϕ are small for this case.

Results for $\varepsilon a = 0.5$ for the case, where the thermal expansion coefficient is larger in the upper part of the FGM layer, are presented in Fig. 9. The values of k_I are much larger than in the previous case for $\varepsilon a = -1$ and for the homogeneous case. The variation of k_I with β is small, the changes of k_{II} with β are larger and for both k_I and k_{II} are almost linear. The variation of ϕ (Fig. 9) is similar to the previous cases.

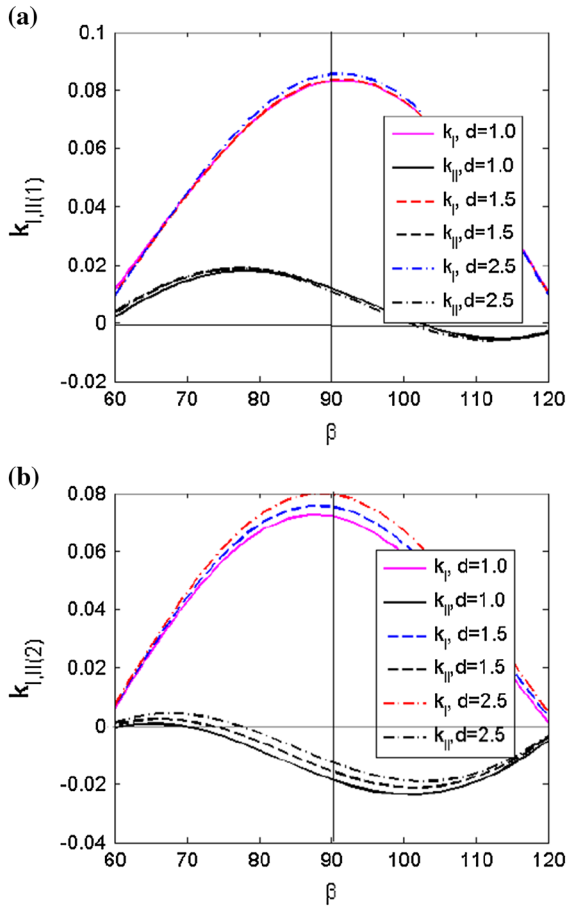

Fig. 11 SIFs k_I and k_{II} as function of the angle β ($\beta_n = \beta$, n = 1, 2) for two edge cracks: **a** for crack 1, **b** for crack 2; for $\varepsilon a = -0.3$. Thermo-mechanical loading

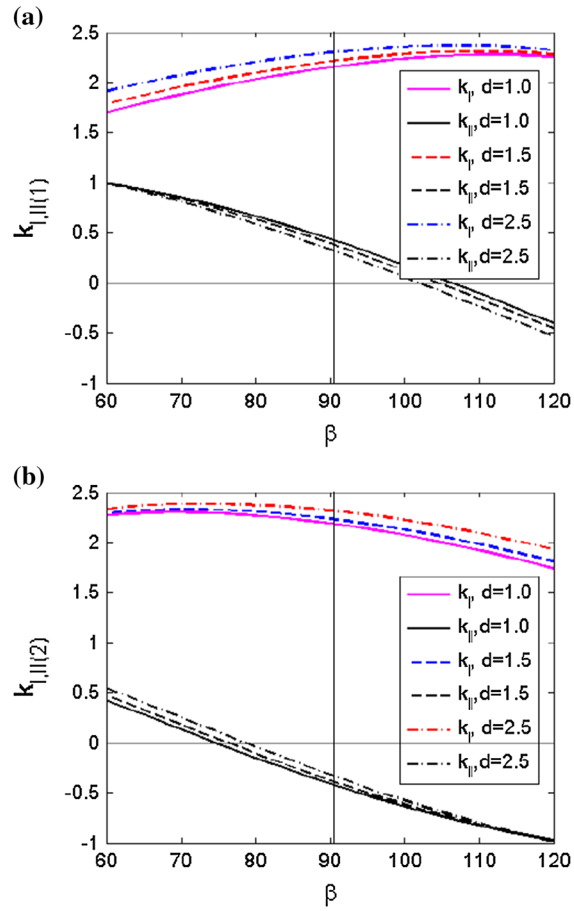

Fig. 12 SIFs k_I and k_{II} as function of the angle β ($\beta_n = \beta$, n = 1, 2) for two edge cracks: **a** for crack 1, **b** for crack 2; for $\varepsilon a = 0.3$. Thermo-mechanical loading

4.2.3 *Inhomogeneous material, thermal and mechanical loadings*

For this case

$$\begin{aligned} p + p^* &= p + \sigma^e_{xx} + \sigma^T_{xx} = p\ \exp(\delta(h + y^0_k)) \\ &\quad \exp(-\delta x_k \sin\beta_k) \\ &\quad +\ Q[\exp(\varepsilon(h + y^0_k))\exp(-\varepsilon x_k \sin\beta_k) - 1]\ ] \\ &= Q[p/Q\ \exp(\delta(h + y^0_k))\exp(-\delta x_k \sin\beta_k) \\ &\quad +\ \exp(\varepsilon(h + y^0_k))\exp(-\varepsilon x_k \sin\beta_k) - 1]. \end{aligned} \tag{21}$$

For simplicity of the parametric analysis we assume that the inhomogeneity parameters ε and δ (of the thermal expansion coefficient and the Young's modulus, correspondingly) are equal and, besides, $p = Q$ as it was in the previous case for thermally inhomogeneous materials.

Figures 11 and 12 show the results of calculation of the non-dimensional SIFs ($k_{I,II} = K_{I,II}/Q\sqrt{2a}$) for this case of loading. Other parameters are the same as in the previous cases, i.e. $d = 1$, 1.5, 2.5 and h/a = 4. The results for $\varepsilon a = -0.3$, where the thermal expansion coefficient is larger in the upper FGM, are presented in Fig. 11 and they have similar trends as in the thermally inhomogeneous case (Fig. 7, $\varepsilon a = -1$) with very small values of k_I and k_{II}. Figure 12 shows the values of k_I and k_{II} for $\varepsilon a = 0.3$ and these results are similar to the previous case shown in Fig. 9 (for thermally inhomogeneous materials for $\varepsilon a = 0.5$) with slightly different magnitudes of k_I and k_{II}.

5 Conclusions

Theoretical modeling of thermal fracture of a semi-infinite FGM is presented for the case of one cycle of thermo-mechanical loading and can be used as a part of a study of the fracture process in FGM coatings under cyclic heating–cooling thermal loading.

Influence of geometrical and material (inhomogeneity) parameters on the fracture characteristics is investigated. Strong influence of the inhomogeneity parameter εa of the material on SIFs is observed. If εa is negative, which corresponds to smaller values of the thermal expansion coefficient in the upper part of the FGM layer, the SIFs k_I and k_{II} at the edge crack tips are small and have much smaller values in comparison to the homogeneous material. For positive εa, the case where magnitudes of the thermal expansion coefficient have larger values in the upper part of the FGM layer, the SIF k_I is much larger than the values for the negative εa and for a homogeneous material. The magnitude of SIF k_{II} is also larger, but not so much as for k_I. The fracture angles have similar tendencies for all considered cases and depend mainly on the inclination angle of the cracks to the boundary. The maximum circumferential stress criterion was applied and probably other criteria should be used in order to take into account the inhomogeneity material properties. For example, the strain energy density criterion [28] includes material parameters and can get more results with respect to the fracture angle prediction.

Acknowledgments The research leading to these results has received funding from the European Union Seventh Framework Programme (FP7/2007–2013), FP7—REGPOT–2009–1, under grant agreement No: 245479; CEMCAST. The support by Polish Ministry of Science and Higher Education—Grant No 1471-1/7.PR UE/2010/7—is also acknowledged.

Appendix

The regular kernels R_{nk}(t,x) and $S_{nk}(t,x)$ contain geometry of the problem and are written as

$$R_{nk}(t,x) = (1-\delta_{nk})K_{nk}(t,x) + \frac{e^{i\alpha_k}}{2}\left\{\frac{1}{X_n-\bar{T}_k} + \frac{e^{-2i\alpha_n}}{\bar{X}_n-T_k} + \right.$$
$$\left. + (\bar{T}_k - T_k)\left[\frac{1+e^{-2i\alpha_n}}{(\bar{X}_n-T_k)^2} - \frac{2e^{-2i\alpha_n}(X_n-T_k)}{(\bar{X}_n-T_k)^3}\right]\right\}, \quad (22)$$

$$S_{nk}(t,x) = (1-\delta_{nk})L_{nk}(t,x) + \frac{e^{-i\alpha_k}}{2}\left[\frac{T_k-\bar{T}_k}{(X_n-\bar{T}_k)^2} + \frac{1}{\bar{X}_n-T_k} - e^{-2i\alpha_n}\frac{X_n-T_k}{(\bar{X}_n-T_k)^2}\right], \quad (23)$$

$$T_k = te^{i\alpha_k} + z_k^0,\ X_n = xe^{i\alpha_n} + z_n^0,\ n,k = 1,2. \quad (24)$$

and

$$\delta_{nk} = \begin{cases} 0 & for\ n \neq k; \\ 1 & for\ n = k. \end{cases}$$

The kernels K_{nk}(t,x) and L_{nk}(t,x) are

$$K_{nk}(t,x) = \frac{e^{i\alpha_k}}{2}\left(\frac{1}{T_k-X_n} + \frac{e^{-2i\alpha_n}}{\overline{T}_k-\overline{X}_n}\right), \quad (25)$$

$$L_{nk}(t,x) = \frac{e^{-i\alpha_k}}{2}\left(\frac{1}{\overline{T}_k-\overline{X}_n} + \frac{T_k-X_n}{(\overline{T}_k-\overline{X}_n)^2}e^{-2i\alpha_n}\right). \quad (26)$$

They are the same as for the system of cracks in an infinite plane. The additional terms in Eqs. (22) and (23) are taking into account the influence of the edge of half plane. α_n is the inclination angle of n-th crack to the x-axis coincide with the edge of the half plane and $\alpha_n = -\beta_n$, Fig. 1; z_n^0 is the coordinate of the center of crack in the global coordinate system (x,y).

References

1. Miyamoto Y, Kaysser WA, Rabin BH (1999) Functionally graded materials: design, processing and applications. Kluwer, Netherlands
2. Birman V, Byrd LW (2007) Modeling and analysis of functionally graded materials and structures. ASME Appl Mech Rev 60:195–216
3. Sadowski T (2008) Non-symmetric thermal shock in ceramic matrix composite (CMC) materials. In: de Bost R, Sadowski T (eds) Lecture notes on composite materials—current topics and achievements. Springer, Berlin, pp 99–148
4. Kawasaki A, Watanabe R (2002) Thermal fracture behavior of metal/ceramic functionally graded materials. Eng Fract Mech 69:1713–1728

5. Shukla A, Jain N, Chona R (2007) A review of dynamic fracture studies in functionally graded materials. Strain 43:76–95
6. Qian G, Nakamura T, Berndt CC (1998) Effects of thermal gradient and residual stresses on thermal barrier coating fracture. Mech Mater 27:91–110
7. Anlas G, Santare MH, Lambros J (2000) Numerical calculation of stress intensity factors in functionally graded materials. Int J Fract 104:131–143
8. Anlas G, Lambros J, Santare MH (2002) Dominance of asymptotic crack tip fields in elastic functionally graded materials. Int J Fract 115:193–204
9. Afsar AM, Sekine H (2000) Crack spacing effect on the brittle fracture characteristics of semi-infinite functionally graded materials with periodic edge cracks. Int J Fract 102:L61–L66
10. Noda N-A, Oda K (1992) Numerical solution of the singular integral equations in the crack analysis using the body force method. Int J Fract 58:285–304
11. Yıldırım B, Özge Kutlu, Kadıoglu S (2011) Periodic crack problem for a functionally graded half-plane an analytic solution. Int J Solids Struct 48:3020–3031
12. El-Borgi S, Djemel MF, Abdelmoula R (2008) A surface crack in a graded coating bonded to a homogeneous substrate under thermal loading. J Therm Stresses 31:176–194
13. Petrova V, Schmauder S (2012) Interaction of a system of cracks with an interface crack in functionally graded/homogeneous bimaterials under thermo-mechanical loading. Comp Mater Sci 64:229–233
14. Petrova V, Schmauder S (2014) Modelling of thermal fracture of functionally graded/homogeneous bimaterial structures under thermo-mechanical loading. Key Eng Mater 592–593:145–148
15. Sadowski T, Neubrand A (2004) Estimation of the crack length after thermal shock in FGM strip. Int J Fract 127:L135–L140
16. Sladek J, Sladek V, Zhang Ch (2005) An advanced numerical method for computing elastodynamic fracture parameters in functionally graded materials. Comp Mater Sci 32:532–543
17. Afsar AM, Sekine H (2002) Inverse problems of material distributions for prescribed apparent fracture toughness in FGM coating around a circular hole in infinite elastic media. Compos Sci Technol 62:1063–1077
18. Petrova V, Sadowski T (2012) Theoretical modeling and analysis of Mode II cracks in Compact Shear specimens. In: ECCOMAS 2012—European congress on computational methods in applied sciences and engineering, e-Book Full Papers, pp. 2601–2611
19. Erdogan F, Wu BH (1997) The surface crack problem for a plate with functionally graded properties. ASME J Appl Mech 64:449–456
20. Erdogan F, Wu BH (1996) Crack problems in FGM layers under thermal stresses. J Therm Stress 19:237–265
21. Panasyuk V, Savruk M, Datsyshin A (1976) Stress distribution near cracks in plates and shells (Russian). Naukova Dumka, Kiev
22. Savruk MP (1981) Two-dimensional problems of elasticity for body with cracks (Russian). Naukova Dumka, Kiev
23. Erdogan F, Gupta G (1972) On the numerical solution of singular integral equations. Quart Appl Math 29:525–534
24. Murakami Y (ed) (1987) Stress intensity factors handbook. In 2 vol, Pergamon press, Oxford etc
25. Freese CE (1976) Periodic edge cracks of unequal length in a semi-infinite tensile sheet. Int J Fract 12:125–134
26. Shackelford JF, Alexander W (2001) CRC materials science and engineering handbook. CRC Press, Boca Raton
27. Erdogan F, Sih GC (1963) On the crack extension in plates under plane loading and transverse shear. J Basic Eng 85:519–527
28. Sih GC (1974) Strain-energy-density factor applied to mixed-mode crack problems. Int J Fract 10:305–321